Supplementary Information

Coupling Cu doping and oxygen vacancies in Co$_3$O$_4$ for efficient electrochemical nitrate conversion to ammonia

Bo Li, [a] Pengfei Xue, [a] Yu Bai, [a] Qin Tang, [b] Man Qiao, [a] and Dongdong Zhu *[a]

[a] School of Chemistry and Materials Science, Institute of Advanced Materials and Flexible Electronics (IAMFE), Nanjing University of Information Science and Technology, Nanjing, 210044, China
E-mail: dd.zhu@nuist.edu.cn

[b] School of Chemistry and Chemical Engineering, Yancheng Institute of Technology, Yancheng, China

1. Experimental section

1.1 Materials: Cobalt nitrate hexahydrate ($Co(NO_3)_2·6H_2O$), urea ($CO(NH_2)_2$), ammonium fluoride (NH_4F), Sodium nitrate ($NaNO_3$), sodium nitrite ($NaNO_2$), sodium sulfate (Na_2SO_4), ammonium chloride (NH_4Cl), sodium salicylate ($C_7H_5N_aO_3$), trisodium citrate dihydrate ($C_6H_5Na_3O_7·2H_2O$), ammonium chloride (NH_4Cl), sodium hydroxide ($NaOH$), sodium nitroferricyanide dihydrate ($C_5FeN_6Na_2O·2H_2O$), sulfamic acid solution (H_3NO_3S), sodium hypochlorite solution ($NaClO$), Copper(II) Chloride Dihydrate ($CuCl_2·2H_2O$), and N-(1-naphthyl) ethylenediamine dihydrochloride ($C_{12}H_{14}N_2$) were purchased from Aladdin Ltd. (Shanghai, China). Sulfuric acid (H_2SO_4), hydrogen peroxide (H_2O_2), hydrochloric acid (HCl) and ethanol (C_2H_5OH) were bought from China National Pharmaceutical Group Corp. (China). All reagents used in this work were analytical grade without further purification.

1.2 Preparation of Cu-Co$_3$O$_{4-x}$, Cu-Co$_3$O$_4$ and Co$_3$O$_4$: Cu-Co$_3$O$_{4-x}$ nanowire grown on CC was prepared as following: Firstly, 2.5 mmol of $Co(NO_3)_2·6H_2O$, 5.0 mmol of NH_4F and 12.5 mmol of urea were dissolved in 35.0 mL deionized water. After the solution was stirred for 5 mins, the pre-treated CC ($3 × 3$ cm^2) substrate was immersed into the solution and transferred into a 50.0 mL Teflon-lined autoclave. The autoclave was then sealed and maintained at 120 °C for 6 h. When the autoclave cools down to room temperature, the Co-based precursor on CC was washed several times with distilled water and anhydrous ethanol. Secondly, the obtained Co-based precursor was immersed in 10.0 mM CuCl$_2$ solution for 12 h to go through a cation exchange process. After ion exchange, the product was dried at 60 °C for 2 h, and then annealed in air at 400 °C for 2 h to obtain Cu-Co$_3$O$_4$ sample. Finally, in-situ electrochemical reduction step was carried out on Cu-Co$_3$O$_4$ sample, which was performed with chronoamperometry method at −0.8 V *vs.* RHE in neutral electrolyte for 12 h to obtain Cu-Co$_3$O$_{4-x}$. Co$_3$O$_4$ was prepared via directly annealing Co-based precursor in air at 400 °C for 2 h.

1.3 Electrochemical measurements: All electrochemical measurements were carried out in a H-type electrolytic cell separated by a treated Nafion 117 membrane using the CHI 760E electrochemical workstation (Shanghai, Chenhua) under the ambient conditions. The Cu-Co$_3$O$_4$ ($0.5 × 0.5$ cm^2), saturated calomel electrode (SCE), and platinum foil were used as the working

electrode, reference electrode and counter electrode, respectively. The electrolyte used in both the cathode and anode was 0.25 M Na_2SO_4 with different concentrations of NO_3^-. A stir bar was used in the H-type cell with a stirring rate of 350 rpm to minimize the mass transfer limitation. All the potentials were converted to the reversible hydrogen electrode (RHE). The chronoamperometry test was performed at different potentials for 1.0 h. We collected the product data for three times at each fixed potential, then the average results were obtained and used.

1.4 Determination of NH₃: Concentration of produced NH_3 was quantitatively determined by the indophenol blue method. In brief, 5.0 g of sodium salicylate and 5.0 g of trisodium citrate dihydrate were dissolved in 100.0 mL of 1.0 M NaOH (Reagent A). Reagent B is then configured with 0.05 M NaClO. 0.20 g of sodium nitroferricyanide was dissolved in 20.0 mL of deionized water (Reagent C). 2 mL of the diluted catholyte was obtained from the cathodic chamber and mixed with 2.0 mL of Reagent A, 1.0 mL of Reagent B and 0.20 mL of Reagent C. After standing for 2 h at room temperature, the ultraviolet-visible absorbance was measured at 655 nm. The concentration-absorbance calibration curve was obtained using standard NH_4Cl solution with varying concentration.

1.5 Determination of NO₂⁻: For chromogenic reagent preparation, 0.50 g of sulfanilamide was dissolved in 50.0 mL of 2.0 M HCl solution to prepare sulfanilamide solution (reagent A) and 20.0 mg of N-(1-Naphthyl) ethylenediamine dihydrochloride was dissolved in 20.0 mL of deionized water (reagent B). A certain amount of electrolyte was removed from the electrolytic cell and diluted to 5.0 mL to detection range. Then, 0.1 mL of reagent A were immersed into the dilution solution (5.0 mL). After standing for 10 minutes, 0.1 mL of reagent B were immersed into the aforementioned solution. After standing for 30 minutes at room temperature, the ultraviolet-visible absorption was measured at a wavelength of 540 nm and 650 nm. The final absorbance value is difference at 540 nm and 650 nm. The concentration-absorbance calibration curve was obtained using standard $NaNO_2$ solution with varying concentration.

1.6 Calculations of FE and yield of NH$_3$:

FE = (8 × F ×[NH$_3$] × V) / (M$_{NH3}$ × Q) × 100%

NH$_3$ yield = ([NH$_3$] × V) / ((M$_{NH3}$ × t × S)

Where F is the Faradic constant (96485 C mol^{-1}), [NH$_3$] is the measured NH$_3$ concentration, V is the volume of electrolyte in the anode compartment (40 mL), M$_{NH3}$ is the molar mass of NH$_3$, Q is the total quantity of applied electricity, t is the electrolysis time (1.0 h), S is the loaded area of catalyst (0.5 × 0.5 cm^2).

2. Supplementary Figures and Tables
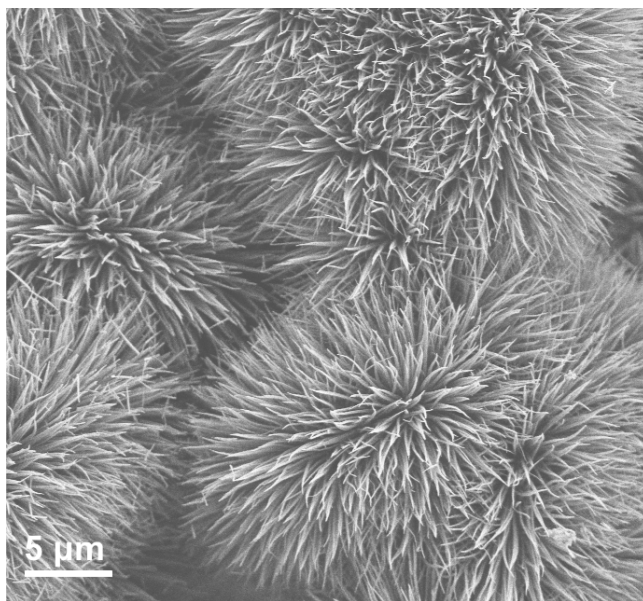
Figure S1. SEM image of Co_3O_4.
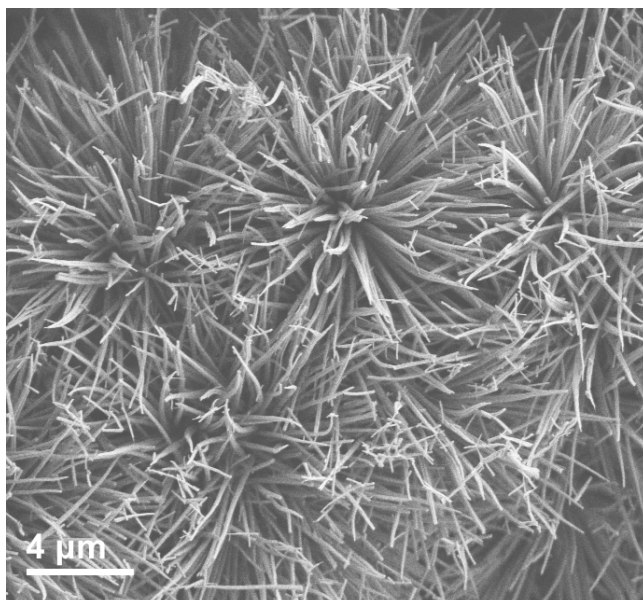
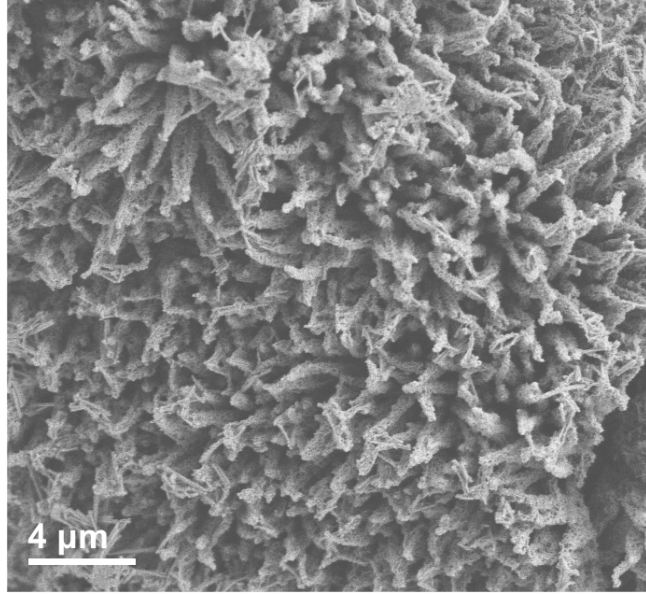Figure S2. SEM image of $Cu\text{-}Co_3O_4$.

Figure S3. SEM image of Cu-Co$_3$O$_{4-x}$.

(a)

A=0.2637c+0.0076
R^2=0.9994
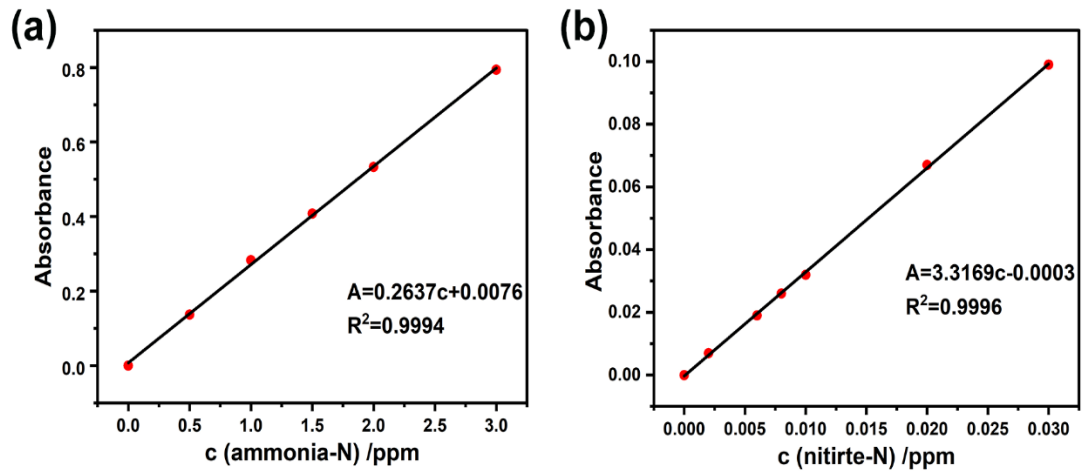
(b)

A=3.3169c-0.0003
R^2=0.9996

Figure S4. The concentration-absorbance calibration curves of (a) ammonia-N, (b) nitrite-N.
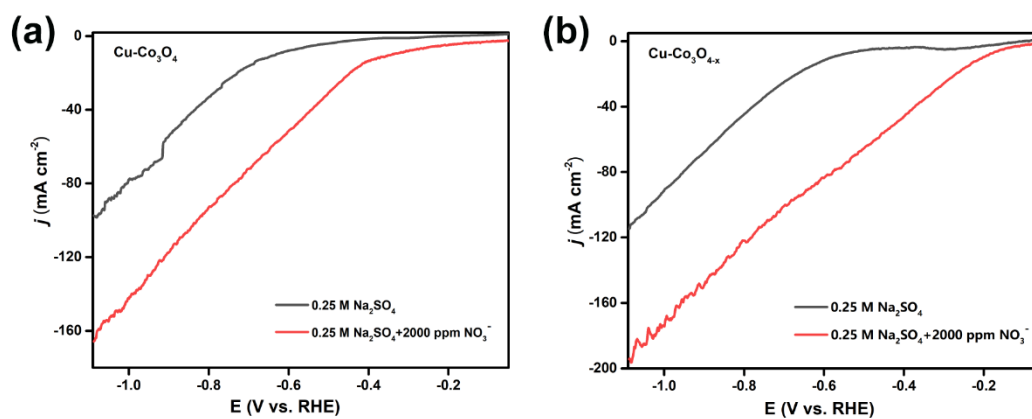
Figure S5. (a) LSV curves of Cu-Co$_3$O$_4$ tested in 0.25 M Na$_2$SO$_4$ with or without 2000 ppm NO$_3^-$, (b) LSV curves of Cu-Co$_3$O$_{4-x}$ tested in 0.25 M Na$_2$SO$_4$ with or without 2000 ppm NO$_3^-$.
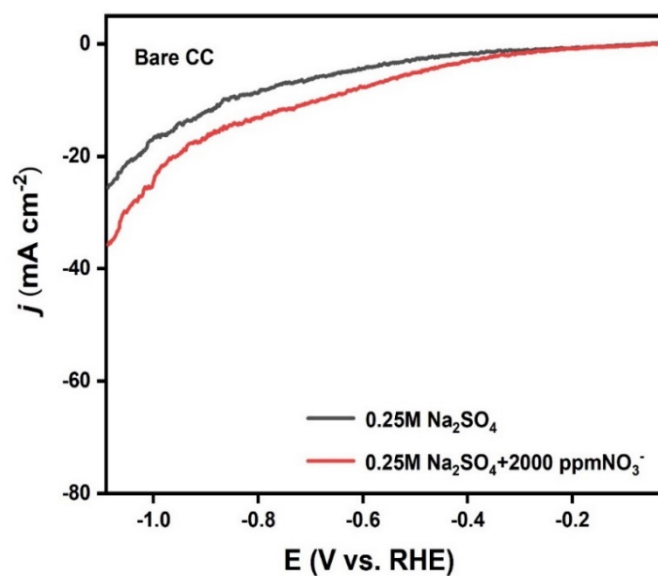

Figure S6. LSV curves of bare CC tested in 0.25 M Na$_2$SO$_4$ with or without 2000 ppm NO$_3^-$.
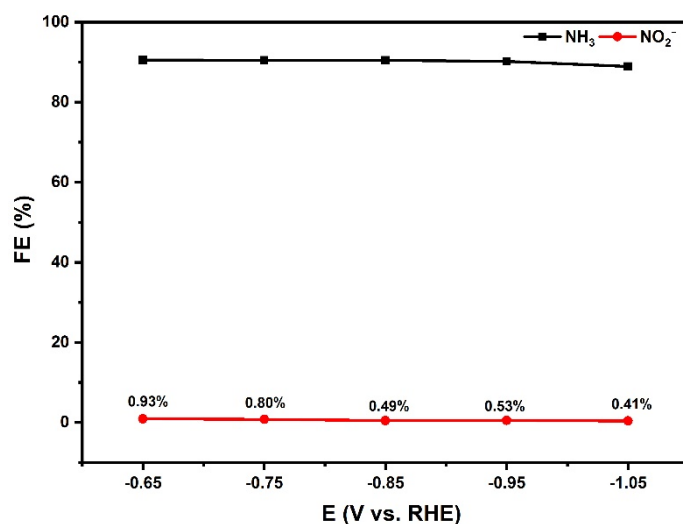
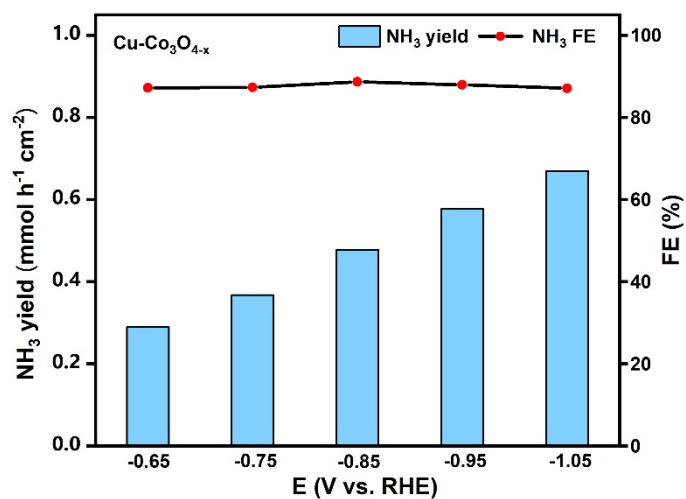Figure S7. FEs of NH_3, and NO_2^- on Cu-Co_3O_{4-x} at different applied potentials.

Figure S8. NH_3 yields and FEs of Cu-Co_3O_{4-x} sample prepared via changing the in-situ electrochemical reduction time to 24 hours at different applied potentials in 0.25 M Na_2SO_4 with 2000 ppm NO_3^-. Though the NO_3RR performance of the obtained Cu-Co_3O_{4-x} sample is slightly worse than the Cu-Co_3O_{4-x} sample prepared via 12-hour in-situ electrochemical reduction, it is still better than Cu-Co_3O_4 sample, highlighting the importance of oxygen vacancies.
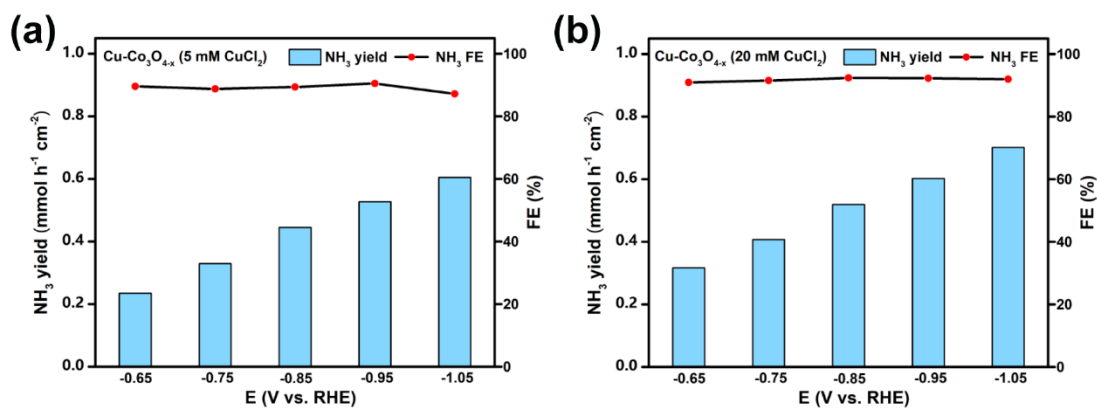
Figure S9. NH$_3$ yields and FEs of Cu-Co$_3$O$_{4-x}$ samples with different Cu content prepared via using (a) 5 mM CuCl$_2$, and (b) 20 mM CuCl$_2$ solution in the cation exchange step at different applied potentials in 0.25 M Na$_2$SO$_4$ with 2000 ppm NO$_3^-$.

Figure S10. (a) Cyclic voltammograms (CV) curves for Cu-Co$_3$O$_{4-x}$ at the scan rates from 20 to 100 mV s^{-1}. (b) Current density as a function of the scan rate to give the double-layer capacitance (C$_{dl}$) for Cu-Co$_3$O$_{4-x}$.
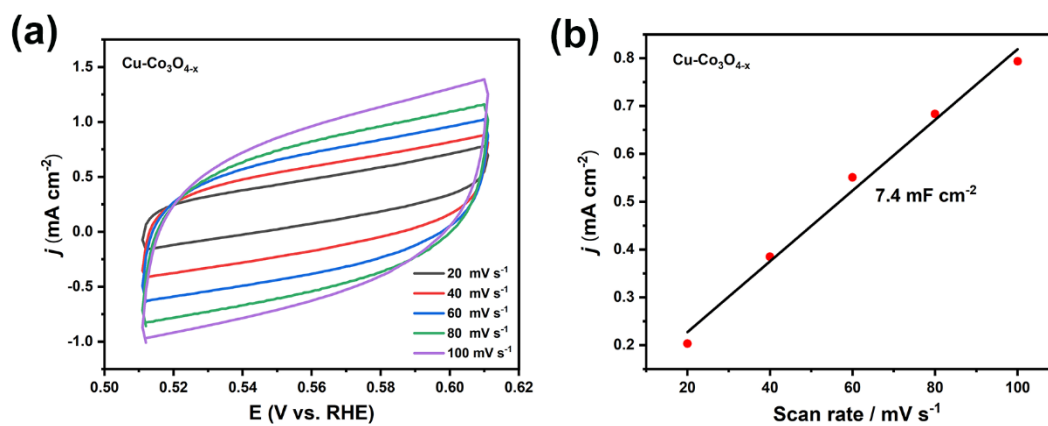
Figure S11. (a) Cyclic voltammograms (CV) curves for Cu-Co$_3$O$_4$ at the scan rates from 20 to 100 mV s^{-1}. (b) Current density as a function of the scan rate to give the double-layer capacitance (C$_{dl}$) for Cu-Co$_3$O$_4$.

Figure S12. (a) Cyclic voltammograms (CV) curves for Co$_3$O$_4$ at the scan rates from 20 to 100 mV s^{-1}. (b) Current density as a function of the scan rate to give the double-layer capacitance (C$_{dl}$) for Co$_3$O$_4$.
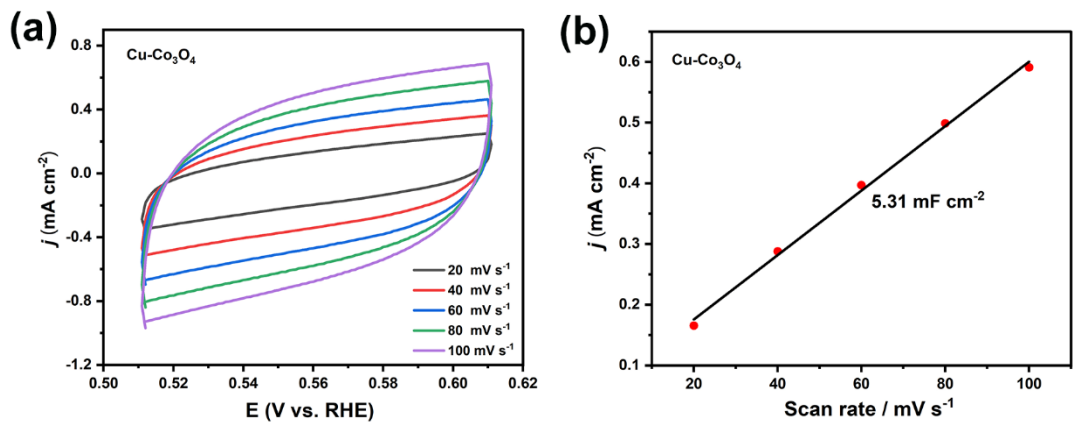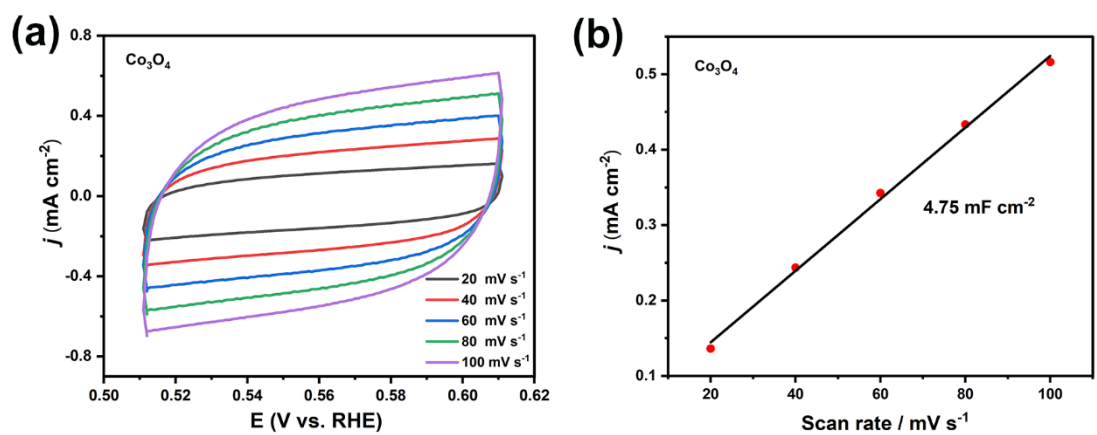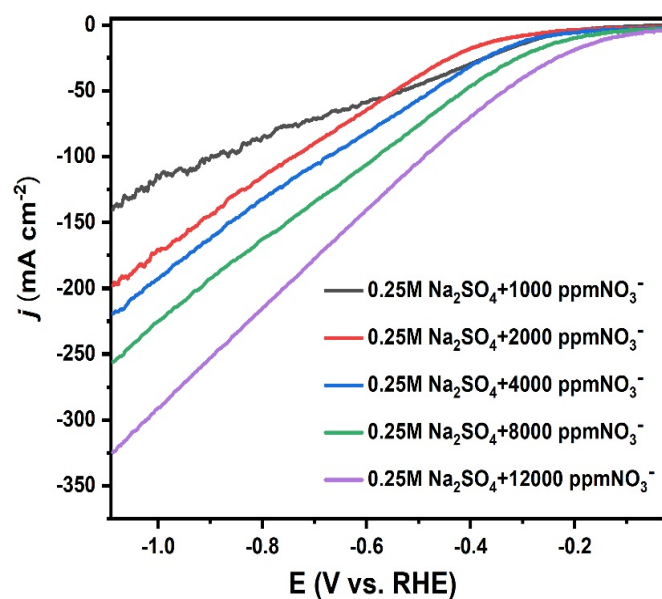
Figure S13. LSV curves of Cu-Co$_3$O$_{4-x}$ tested with different NO$_3^-$ concentrations.
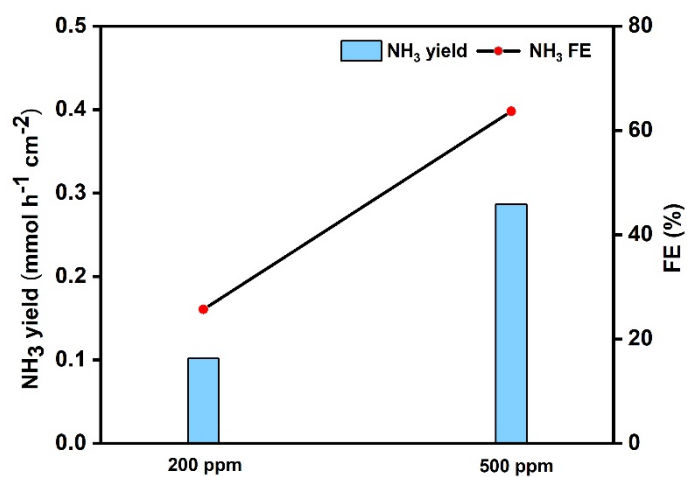

Figure S14. NH$_3$ yields and FEs of Cu-Co$_3$O$_{4-x}$ tested at –0.95V *vs.* RHE in 0.25 M Na$_2$SO$_4$ with low NO$_3^-$ concentrations.
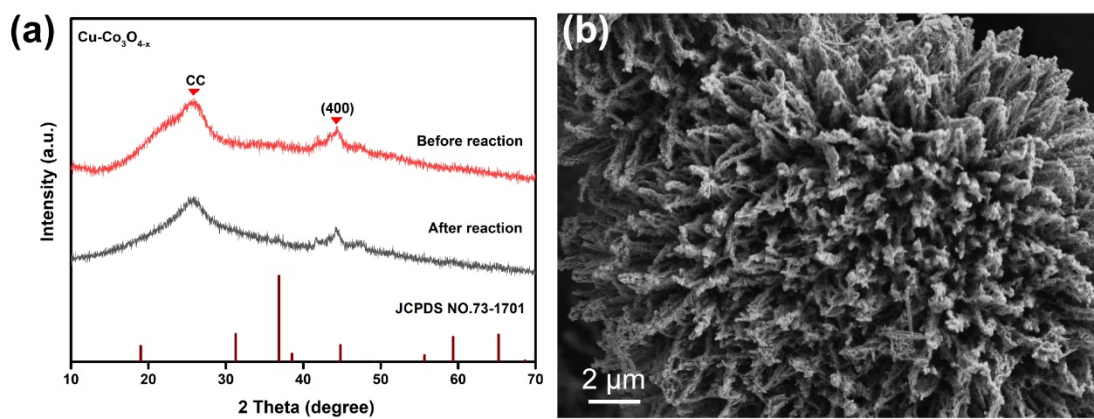
Figure S15. (a) XRD patterns of Cu-Co$_3$O$_{4-x}$ sample before and after the NO$_3$RR cycling test, (b) SEM image of Cu-Co$_3$O$_{4-x}$ sample after the NO$_3$RR cycling test. The XRD results display that the intrinsic structure of Cu-Co$_3$O$_{4-x}$ was well preserved after NO$_3$RR cycling test, as the significant (400) peak of Co$_3$O$_4$ can be clearly observed. The SEM image shows that the nanoarray configuration of Cu-Co$_3$O$_{4-x}$ was maintained after the cycling test.

Table S1. Summary of the performance of recently reported NO_3RR electrocatalysts in the neutral electrolytes.

Catalyst	Electrolyte	Potential	Performance	Ref.
Cu-Co$_3$O$_{4-x}$	0.25 M Na$_2$SO$_4$ 2000 ppm NO$_3^-$	−1.05 V (V *vs.* RHE)	FE = 88.9% NH$_3$ yield = 0.83 mmol h^{-1} cm^{-2}	This work
TiO$_{2-x}$	0.50 M Na$_2$SO$_4$ 0.50 mg L^{-1} NO$_3^-$	−1.6 V (V *vs.* SCE)	FE = 85% NH$_3$ yield = 0.045 mmol h^{-1} mg^{-1}	1
Cu/Cu$_2$O	0.50 M Na$_2$SO$_4$ 200 ppm NO$_3^-$	−0.85 V (V *vs.* RHE)	FE = 95.8% NH$_3$ yield = 0.245 mmol h^{-1} cm^{-2}	2
Fe SAC	0.10 M K$_2$SO$_4$ 0.50 M KNO$_3$	−0.66 V (V *vs.* RHE)	FE = 75% NH$_3$ yield = 0.46 mmol h^{-1} cm^{-2}	3
Co/CoO NSA	0.10 M K$_2$SO$_4$ 200 ppm NO$_3^-$	−1.3 V (V *vs.* SCE)	FE = 93.8% NH$_3$ yield = 0.20 mmol h^{-1} cm^{-2}	4
Co$_3$O4/NiO HNTs	0.50 M Na$_2$SO$_4$ 200 ppm NO$_3^-$	−0.8 V (V *vs.* RHE)	FE = 55% NH$_3$ yield = 6.9 mmol h^{-1} g^{-1}	5
Pd$_{Octohedron}$	0.10 M Na$_2$SO$_4$ 0.10 M NO$_3^-$	−0.7 V (V *vs.* RHE)	FE = 79.91% NH$_3$ yield = 0.549 mmol h^{-1} cm^{-2}	6
Cu-PTCDA	0.10 M PBS 500 ppm NO$_3^-$	−0.4 V (V *vs.* RHE)	FE = 85.9% NH$_3$ yield = 436 µg h^{-1} cm^{-2}	7
Fe–SnS$_2$	0.50 M Na$_2$SO$_4$ 0.10 M NO$_3^-$	−0.7 V (V *vs.* RHE)	FE = 85.6% NH$_3$ yield = 7.2 mg h^{-1} cm^{-2}	8
B–MoS$_2$	0.50 M Na$_2$SO$_4$ 0.10 M NO$_3^-$	−0.7 V (V *vs.* RHE)	FE = 92.3% NH$_3$ yield = 10.8 mg h^{-1} cm^{-2}	9
meso-PdN NCs	0.10 M Na$_2$SO$_4$ 0.005 M NO$_3^-$	−0.7 V (V *vs.* RHE)	FE = 96.1% NH$_3$ yield = 3760 µg h^{-1} mg^{-1}	10

References

1   R. Jia, Y. Wang, C. Wang, Y. Ling, Y. Yu and B. Zhang, *ACS Catal.*, 2020, **10**, 3533-3540.

2   Y. Wang, W. Zhou, R. Jia, Y. Yu and B. Zhang, *Angew. Chem. Int. Ed.*, 2020, **59**, 5350-5354.

3   Z.-Y. Wu, M. Karamad, X. Yong, Q. Huang, D. A. Cullen, P. Zhu, C. Xia, Q. Xiao, M. Shakouri, F.-Y. Chen, J. Y. Kim, Y. Xia, K. Heck, Y. Hu, M. S. Wong, Q. Li, I. Gates, S. Siahrostami and H. Wang, *Nat. Commun.*, 2021, **12**, 2870.

4   Y. Yu, C. Wang, Y. Yu, Y. Wang and B. Zhang, *Sci. China Chem.*, 2020, **63**, 1469-1476.

5   Y. Wang, C. Liu, B. Zhang and Y. Yu, *Sci. China Mater.*, 2020, **63**.

6   Y. Han, X. Zhang, W. Cai, H. Zhao, Y. Zhang, Y. Sun, Z. Hu, S. Li, J. Lai and L. Wang, *J. Colloid Interface Sci.*, 2021, **600**, 620-628.

7   G.-F. Chen, Y. Yuan, H. Jiang, S.-Y. Ren, L.-X. Ding, L. Ma, T. Wu, J. Lu and H. Wang, *Nat. Energy*, 2020, **5**, 605-613.

8   K. Chen, Y. Luo, P. Shen, X. Liu, X. Li, X. Li and K. Chu, *Dalton Trans.*, 2022, **51**, 10343-10350.

9   Y. Luo, K. Chen, P. Shen, X. Li, X. Li, Y. Li and K. Chu, *J. Colloid Interface Sci.*, 2023, **629**, 950-957.

10   L. Sun and B. Liu, *Adv. Mater.*, 2023, **35**, 2207305.